[9] Vidal, R. J. and Bartz, J. A., "Surface Measurements on Sharp Flat Plates and Wedges in Low Density Hypersonic Flow," CAL AF-2041-A-2, 1968, Cornell Aeronautical Lab., Buffalo, N. Y.

[10] Probstein, R. F. and Elliott, D., "The Transverse Curvature Effect in Compressible Axially Symmetric Laminar Boundary Layer Flow," *Journal of the Aeronautical Sciences*, Vol. 23, No. 3, March 1956, p. 208.

[11] Oguchi, H., "Leading Edge Slip Effects in Rarefied Hypersonic Flow," *Rarefied Gas Dynamics*, Supplement 2, Vol. II, edited by J. A. Laurmann, Academic Press, New York, 1963, pp. 181–193.

[12] TR 1135, 1953, NACA.

[13] Hayes, W. D. and Probstein, R. F., *Hypersonic Flow Theory*, Academic Press, New York, 1959.

[14] McCroskey, W. J., Bogdonoff, S. M., and Genchi, A. P., "Leading Edge Flow Studies of Sharp Bodies in Rarefied Hypersonic Flow," *Rarefied Gas Dynamics*, Supplement 4, Vol. II, edited by C. L. Brundin, Academic Press, New York, 1967, pp. 1047–1066.

[15] Vas, I. E., Iacavazzi, C., Carlomagno, G., and Bogdonoff, S. M., "Effect of Body Inclination on the Merging of a Hypersonic Low Density Flow Over Sharp Two-Dimensional Linear Bodies," *Rarefied Gas Dynamics*, Supplement 5, Vol. I, edited by L. Trilling and H. Wachman, Academic Press, New York, 1969, pp. 501–508.

[16] Feik, R. A., Genchi, A. and Vas, I. E., "A Study of Merging on Cones," *Rarefied Gas Dynamics*, Supplement 5, Vol. I, edited by L. Trilling and H. Wachman, Academic Press, New York, 1969, pp. 493–499.

[17] Waldron, H. F., "Viscous Hypersonic Flow Over Pointed Cones at Low Reynolds Numbers," *AIAA Journal*, Vol. 5, No. 2, Feb. 1967, pp. 208–218.

[18] Hofland, R. and Glick, H. S., "Low Density Hypersonic Flow Over a Cone," *AIAA Journal*, Vol. 8, No. 1, Jan. 1970, pp. 52–59.

[19] Mirels, H. and Ellinwood, J. W., "Hypersonic Viscous Interaction Theory for Slender Axisymmetric Bodies," *AIAA Journal*, Vol. 6, No. 11, Nov. 1968, pp. 2061–2070.

SEPTEMBER 1972 AIAA JOURNAL VOL. 10, NO. 9

Jet Impingement under VTOL Aircraft

THOMAS M. HOULIHAN* AND CHARLES D. THOMPSON†
Naval Postgraduate School, Montery, Calif.

A previous analytical solution for the flowfield beneath a VTOL model was extended to include tilted jet configurations. Additionally, a laboratory model was constructed to test the effects of variation in the parameters governing the flow. Free streamline profiles, pressure coefficients on the "ground" and "fuselage" of the apparatus and velocity profiles in the nozzles were determined from hot wire anemometer traverses of the flowfield. Experimental data compared favorably with theoretical determinations over the flow regions tested.

Nomenclature

C_p = pressure coefficient
K = complete elliptic integral of the first kind
K' = defined by $K'(k) \equiv K(k')$
k = modulus of elliptic integral
k' = defined as $(1 - k^2)^{1/2}$
R_e = Reynolds number, $\Delta V_0/\nu$
T = complex variable in T-plane, $\xi + i\eta$
V_I = velocity at nozzle exit
$\bar{V}_I$ = average velocity at nozzle exit
V_0 = velocity along free streamlines
W = complex potential, $\Phi + i\Psi$
x, y = coordinates in physical plane
z = complex variable, $x + iy$
α = tilt angle of nozzle
β = plate angle
Γ = flow region in the T-plane
Δ = width of nozzle
δ_L, δ_R = asymptotic widths of streams flowing to left and to right
ζ = complex conjugate velocity, $u - iv$
θ = theta-function
ξ, η = coordinates of T-plane
ρ = density
Φ = velocity potential
Ψ = stream function

Subscripts

A, G, H = refer to stagnation points
F = refers to point on fuselage plate
r = refers to boundary point

Introduction

IN recent years, crowded airport facilities, the search for rapid urban transportation, and the need for military aircraft capable of operating from advanced bases, have resulted in a great deal of attention being given to VTOL aircraft. Much research has been performed on various models and full-scale versions of these aircraft. Some operational types have been developed.

When operating near the ground, these aircraft are quite similar in principle to ground effect machines. Ground effect can be either beneficial or detrimental, depending upon the configuration of the aircraft. Land erosion, damage to objects near the operating area, and recirculation of debris and hot exhaust gases beneath the fuselage are some of the problems involved with hovering near the ground. The reingestion of exhaust gases reduces the efficiency of the engines. Recirculating debris may also enter the engines or severely damage the underside of the aircraft. Some pilots have experienced handling difficulties, drastic loss of power, and visibility problems, as a result of ground effect.

The recirculating flow underneath the aircraft, however, can also produce a lifting force which can significantly reduce the thrust necessary to operate the aircraft. Small modifications to the aircraft, such as tilting of engines, can often reduce the unfavorable effects to such an extent that the additional lift provided by the recirculating flow can produce improved performance. In order to estimate the effects of various modifications, a mathematical model of the flowfield beneath VTOL aircraft, incorporating the elements of free streamline theory, was developed. Verification of the primary conclusions of this analysis, together with an investigation of the range of its applicability, is the subject of the following work.

Theoretical Analysis

A theoretical solution to the flowfield beneath a VTOL aircraft was obtained by Goldstein and Siegel.[1] Their determinations for a two-dimensional model of an aircraft with a slot-jet nozzle exhaust in each wing featured a steady, incompressible, inviscid fluid flow. A flat plate at an angle to the vertical represented the "fuselage" in the configuration shown in Fig. 1 and the nozzles were assumed to always be perpendicular to the

Received December 28, 1970; revision received March 20, 1972. Index category: VTOL Aerodynamics.

* Assistant Professor, Department of Mechanical Engineering. Member AIAA.

† Lieutenant, U. S. Navy, Pensacola, Fla.

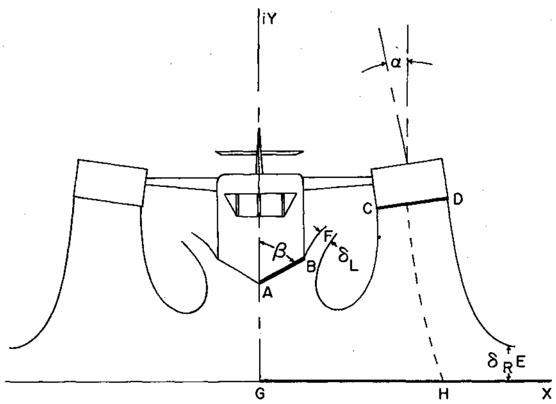

Fig. 1 Physical flowfield.

"ground" of the setup. Since tilting of the nozzles is a possible solution to the recirculation problem existent in VTOL operations, a more general analysis would allow the nozzles to be located at some angle to the vertical. This more general analysis was pursued by Thompson.[2] Proceeding, as did Goldstein and Siegel, the flowfield was mapped into the hodograph and complex potential planes shown in Fig. 2. The hodograph mapping function, which now allowed for tilted nozzles, was

$$\zeta(T) = V_o e^{i(\pi/2-\alpha)}\Omega(\xi_H)[\Omega(\xi_G)]^{1/2}[\Omega(\xi_A)]^{\beta/\pi} \tag{1}$$

where

$$\Omega(\xi_r) = \frac{[\Theta_4(\pi/4K)(T-\xi_r)|(iK'/2K)]}{\Theta_4[(\pi/4K)(T+\xi_r-2K)|(iK'/2K)]}$$

and

$$\Theta_4(z|\tau) = 1 + 2\sum_{n=1}^{\infty}(-1)^n e^{i(\pi/n^2\tau)}\cos 2nz$$

Taking the argument of the function in Eq. (1) and requiring that the direction of the flow along the "fuselage" plate be equal to this argument yielded

$$(4K/\pi)(\pi/4+\alpha+\beta/2) = 2\xi_H + \xi_G + (2\beta/\pi)\xi_A \tag{2}$$

From this point the remainder of the solution followed closely from determinations analogous to those accomplished in Ref. 1. Thus, the final solution for the displacement in the flowfield became

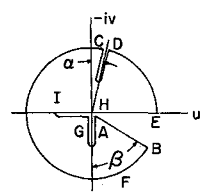

Fig. 2a Hodograph plane.

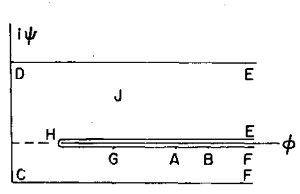

Fig. 2b Complex potential plane.

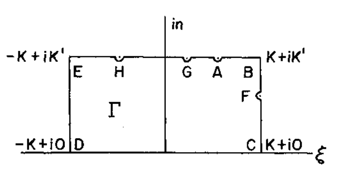

Fig. 2c Integration (T) plane.

$$\frac{z}{\Delta} = C\int_{\xi+ik}^{T}\frac{(k\sin\xi_H snT-1)(1-k\,snT)dT}{dnT[1-dn(\eta_F,k')snT]F}$$

$$C = (V_I/V_0)e^{i\alpha}(k'/\pi)[(sn(\eta_F,k') + \delta_R/\delta_L)/(1+\delta_R/\delta_L)]$$

$$F = \Omega(\xi_H)[\Omega(\xi_G)]^{1/2}[\Omega(\xi_A)]^{\beta/\pi}$$

The exponential terms involving α are the terms added to the original solution by the assumption of a tilted nozzle configuration.

There are six parameters in this solution which determine the flowfield: plate height, plate width, plate angle, nozzle height, nozzle spacing, and nozzle angle. The plate and nozzle angles (α,β) appear explicitly in the solution, while the other four parameters must be calculated.

The solution is determined by an integration along the sides of the rectangular region Γ in the T-plane (Fig. 2). All distances were normalized with respect to the nozzle width. The solution was then evaluated by incorporating the known plate and nozzle angles and the remaining four input parameters ($k, \delta_L/\delta_R, \xi_A/K'$) into the integrations.

Using the working formulae appearing in the appendices of Refs. 3 and 4, two computer programs were developed for the final integral determinations. The first program calculated the plate height and width and the nozzle height and spacing for a given set of input parameters. The second program plotted the theoretical flowfield, the pressure coefficients on the "ground" and "fuselage" plates and the velocity profiles in the nozzles for a series of selected input parameters.

All integrations were performed by the Gauss nine-point quadrature formula and where infinite series were specified, the first five terms of the series were incorporated. The velocity was made negative to fix the downward direction so that the plotted velocity profile was shown as it would appear to one viewing it from in front of the aircraft. Some representative results, together with the corresponding experimental data, are shown in Figs. 5a to 6d.

Experimental Analysis

Air flow at low pressure represented the steady incompressible inviscid flowfield in the apparatus tested. The two-dimensional slot jets were produced by two rectangular nozzles with a cross section length to width ratio of four to one (Fig. 3). By confining all measurements to a plane through the center of the eight-inch nozzles utilized, end effects were rendered negligible.

Each nozzle was attached to the air supply through a diffuser-chamber, housing screening and honeycomb material which ultimately produced a uniform velocity distribution in the nozzle. Rotameters preceded the chambers in the air lines so that the flow conditions could be easily monitored throughout the test period.

A mounting arrangement was designed to not only allow the nozzles to be moved vertically and horizontally, but also to be rotated in the vertical plane, thereby representing a tilted jet

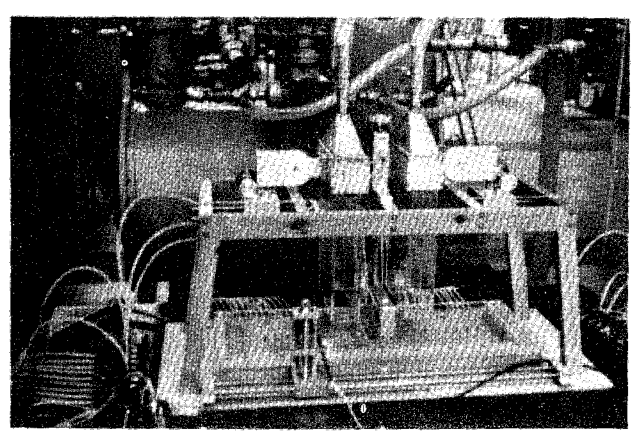

Fig. 3 Laboratory model.

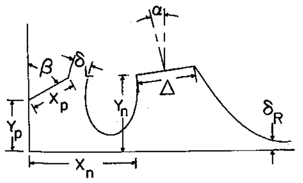

Re	K	$\frac{\delta_L}{\delta}$	$\frac{\eta_F}{K'}$	$\frac{\varepsilon_\Delta}{K}$	β	α	$\frac{X_p}{\Delta}$	$\frac{Y_p}{\Delta}$	$\frac{X_n}{\Delta}$	$\frac{Y_n}{\Delta}$
3900	.3	.3	.6	.2	90	0	.559	.860	.725	1.43
4700	.3	.1	.9	.5	60	10	.422	.863	.460	1.38

Fig. 4 Flowfield parameters.

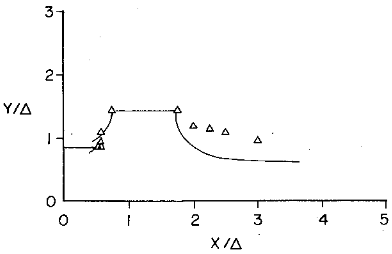

Fig. 5a Freestreamline configuration, $Re = 3900$.

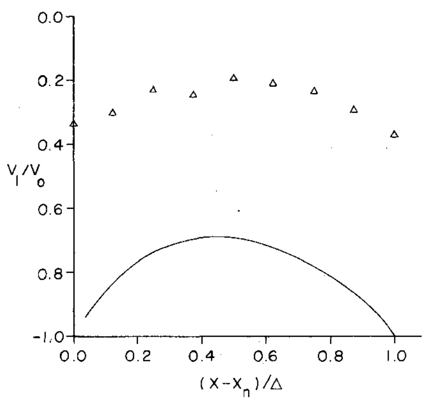

Fig. 5b Nozzle velocity profile, $Re = 3900$.

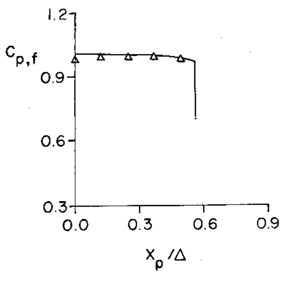

Fig. 5c Fuselage pressure coefficient, $Re = 3900$.

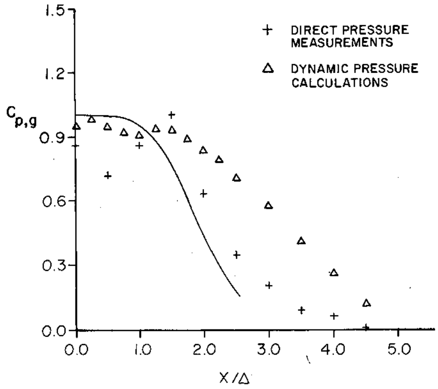

Fig. 5d Ground pressure coefficient, $Re = 3900$.

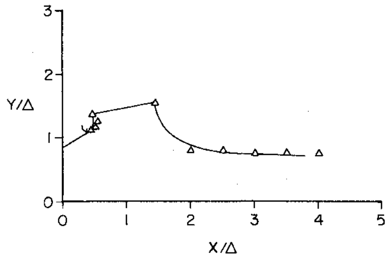

Fig. 6a Freestreamline configuration, $Re = 4700$.

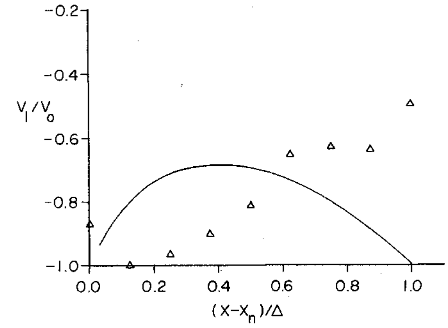

Fig. 6b Nozzle velocity profile, $Re = 4700$.

configuration. Directly underneath the framework and the nozzles was a large plexiglass plate which represented the "ground." Smaller plates representing "fuselages" of various sizes and shapes were made to be interchangeable on a bracket which was suspended from the framework between the nozzles. The vertical position of the plate bracket was varied with a threaded traverse. The ground and the fuselage plates each contained a row of pressure taps across the center of the plates. This enabled direct pressure measurements (+) to be made to corroborate the pressure coefficients (Δ) determined from simultaneous flow velocity measurements.

Tests were run with Reynolds numbers (based upon the velocity and width of the jet) from 1600 to 7000. The data recorded allowed for the plotting of free streamlines of the flowfield, nozzle exit velocity profiles, and pressure coefficients along the fuselage and ground plates (Fig. 4). Some representative results are displayed together with the corresponding theoretical determinations in Figs. 5a to 6d.

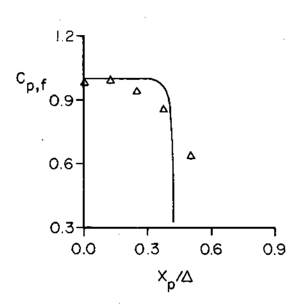

Fig. 6c Fuselage pressure coefficient, $Re = 4700$.

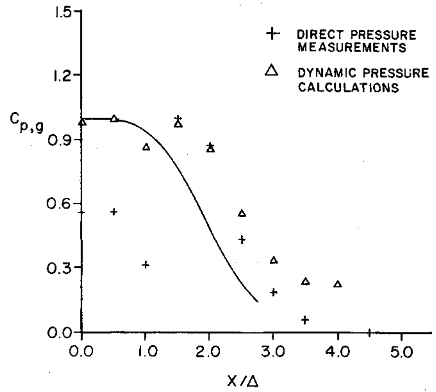

Fig. 6d Ground pressure coefficient, $Re = 4700$.

Discussion of Results

Many combinations of input parameters analytically produced impossible configurations (negative plate heights, etc.) and no combinations were found to produce a configuration with the nozzle exit lower than the plate. Most of the configurations of interest were found to possess input parameters in the following ranges: $0.3 \leqq K \leqq 0.6$, $0.1 \leqq \delta_L/\delta_R \leqq 0.5$, $0.6 \leqq \eta_F/K' \leqq 0.9$, $0.1 \leqq \xi_A/K' \leqq 0.9$.

Possible configurations exited outside of these ranges but most featured extremely small plate widths. Variation of any one input parameter was not found to alter any single physical parameter.

Slight tilting of the nozzles (10°) greatly decreased the flow occurring around the fuselage. Tilting of the nozzles also caused an increase in plate and nozzle heights but decreased plate width and nozzle spacing. Decreasing the plate angle had a tendency to decrease the plate width and increase the plate height. None of these variations had any outstanding effect upon the theoretical pressure coefficients.

Figure 5a displays the encroachment of entrainment effects upon the flowfield extremities for a high nozzle position. It is interesting to note that such entrainment effects do not occur at a high Reynolds number flow (Fig. 6a) for a lower nozzle setting.

Nozzle velocity profiles for low Reynolds number flows closely approximated the theoretical determinations. However, as exit velocities and/or tilt angle increased, the profiles were altered by the nozzle wall presence. In all cases, velocity data were normalized with respect to the maximum velocity for the particular test situation. This maximum velocity occurred near the ground—two to three nozzle widths below the high pressure region between the nozzle exit and fuselage. Hence, the data points are displaced from the theoretical profiles which are based upon the assumption that maximum velocities are reached at the edge of the nozzle exit.

In all the results shown, it is to be noted that the data points in the region between the nozzle and the plate often deviate from the analytical streamline configuration. This is the result of the test plates being of finite thickness, whereas the theoretical plates were infinitely thin plates, i.e., lines. Likewise, the pressure distribution along the ground was not as uniform as that predicted by the analysis because of the finite thicknesses of the nozzle walls.

Summary

Experimental verification of the principal findings in an analysis of the flowfield beneath a VTOL model with a tilted jet configuration has been accomplished. Moreover, the limitations of the theoretical developments vis-a-vis entrainment effects have been demonstrated.

References

[1] Goldstein, M. E. and Siegel, R., "Analysis of Two-Dimensional Inviscid Model of Jet Impingement Under VTOL Aircraft," TN D-5288, 1969, NASA.

[2] Thompson, C. D., "An Investigation of Ground Effect on VTOL Aircraft," thesis, June 1970, Naval Postgraduate School, Monterey, Calif.

[3] Goldstein, M. E. and Siegel, R., "Two Dimensional Inviscid Jet Flow from Two Nozzles at an Angle to a Plane Surface," TN D-5064, 1969, NASA.

[4] Gedney, R. T. and Siegel, R., "Inviscid Flow Analysis of Two Parallel Slot Jets Impinging Normally on a Surface," TN D-4957, 1968, NASA.